Reference: *Biol. Bull.* **193:** 30–46. (August, 1997)

Larval Shell Muscles in the Abalone *Haliotis kamtschatkana*

L. R. PAGE

Department of Biology, University of Victoria, Victoria, British Columbia, Canada V8W 3N5

Abstract. I used light and electron microscopy to investigate shell-attached muscles in larvae of *Haliotis kamtschatkana* Jonas, 1845, because an early description of these muscles in *H. tuberculata* by Crofts (1937, 1955) has featured prominently in theories about gastropod evolution. Larval shell muscles in *H. kamtschatkana* can be grouped into two categories. The first category consists of the larval retractor muscle (LRM) and the accessory larval retractor muscle (ACC); these are striated muscles in which myofilaments begin differentiating before the head and foot rotate relative to the protoconch (this rotation is known as *ontogenetic torsion*). Collectively, these muscles ultimately insert on tissues within the larval head and mantle, but the ACC and mantle fibers of the LRM degenerate as metamorphic competence is achieved. The second category consists of two nonstriated pedal muscles that differentiate after cephalopodial rotation. The left pedal muscle is anchored on the back of the protoconch, to the left of the shell-attachment plaque for the LRM. It projects into the foot primarily, but also gives rise to muscle slips extending into the mantle fold. The right pedal muscle is anchored on a calcareous septum secreted along the visceral rim of the protoconch. The new data force a reconsideration of the ancestral homologues of larval shell muscles in abalone, because Crofts may have misidentified the accessory larval retractor muscle as a precursor of one of the later pedal muscles.

Introduction

The form and development of shell-attached muscles in vetigastropods and patellogastropods, which I will call 'archaeogastropods' (see Hickman, 1988; Haszprunar, 1993), have had considerable impact on theories about early gastropod evolution. Studies by Crofts (1937, 1955) on muscle morphogenesis in *Haliotis tuberculata* and several other archaeogastropods have been particularly influential. Crofts identified two shell muscles in larvae of *H. tuberculata:* the larval (or velar) retractor muscle and the future columellar muscle. She suggested that the precocious differentiation of the larval retractor muscle relative to the columellar muscle initiates the mechanical twisting of the developing larval body known as ontogenetic torsion. Crofts (1937, 1955) also indicated that the pair of larval muscles become the two adult shell muscles in *H. tuberculata*, a condition viewed as primitive within a molluscan class in which most members have only one adult shell muscle. The diagrams in Figure 1A, B depict Crofts' (1937, 1955) interpretation of the larval shell muscles in *H. tuberculata* and several other archaeogastropods during an early and late stage of premetamorphic development.

Crofts' (1937, 1955) descriptions endorsed and extended the hypothesis that the two shell muscles in archaeogastropod larvae, and their postmetamorphic derivatives, are bilateral homologues that have lost their ancestral symmetry (Garstang, 1929). The two are presumed to be descendant remnants of serially duplicated, symmetrical pairs of dorso-ventral shell muscles as retained by extant monoplacophorans and chitons (Knight, 1952; Stasek, 1972; Wingstrand, 1985). This hypothesis has influenced interpretations of paleontological data (see Yochelson, 1967; Harper and Rollins, 1982; Runnegar and Pojeta, 1985) and speculations about evolutionary diversification of shell muscles among extant larval and adult gastropods (Fretter and Graham, 1962; Fretter, 1969; Haszprunar, 1985).

Despite the widespread influence of Crofts' (1937,

Received 2 December 1996; accepted 28 April 1997.

Abbreviations: LRM = larval retractor muscle, ACC = accessory larval retractor muscle.

1955) descriptions of shell muscles in larval archaeogastropods, which were based on paraffin sections, her results have never been confirmed using techniques permitting higher resolution. Indeed, the fact that her descriptions have not consistently coincided with observations by others (Smith, 1935; Bandel, 1982) underlines the need for in-depth study of the development of these muscles. Speculations about ancestry and evolutionary diversification of structures must be based on accurate information about the extant products of structural evolution.

The purpose of my study is not to test the theory claiming a muscle-based mechanism for generating ontogenetic torsion in archaeogastropods, but to reexamine the inventory of larval shell muscles in a haliotid and the fate of these muscles at metamorphosis. Evidence derived from light and transmission electron microscopy of sequential development stages of *Haliotis kamtschatkana* Jonas, 1845, indicates that four, rather than two, shell-attached muscles differentiate during the premetamorphic phase of this species. This interpretation is summarized by the sketches in Figures 1A, C. In particular, I suggest that insufficient resolution and inadequate methods to prevent muscle contraction during fixation may have led Crofts (1937, 1955) to confuse an early developmental stage of a transient muscle projecting to the mantle, with a later differentiating pedal muscle. Observations described in this report extend those given in an earlier study on overall larval morphogenesis of *H. kamtschatkana* (Page, in press), and they indicate that the evolutionary derivation of shell muscles in haliotid gastropods should be reevaluated.

Materials and Methods

Adults of *Haliotis kamtschatkana* were collected from shallow subtidal areas around the southern tip of Vancouver Island, Canada (collection permit obtained from Canadian Department of Fisheries and Oceans), and were induced to spawn by the hydrogen peroxide method of Morse *et al.* (1976). After spawning commenced, adults were rinsed briefly in flowing seawater and transferred to aquaria containing seawater without hydrogen peroxide, where spawning continued. Collected eggs were rinsed with Millipore-filtered seawater (0.45-μm pore size) before and after they were fertilized with a dilute sperm suspension. After larvae hatched, they were maintained in beakers containing 500 ml Millipore-filtered seawater (12° to 13°C), which was changed daily. Antibiotics (streptomycin sulfate at 50 μg/ml and penicillin G at 60 μg/ml; both from Sigma) were added on days 6 and 9 postfertilization. Red coralline algae (*Lithothamnion* sp.) or 0.01 m*M* gamma aminobutyric acid (Sigma) was used to induce metamorphosis of *H. kamtschatkana* larvae (indicated by loss of the ciliated velar cells), as described previously for the congeneric species, *Haliotis rufescens* (Morse *et al.*, 1979; Morse and Morse, 1984).

Larval stages were fixed at the following times after fertilization: 42, 52, 62, 72, and 96 hours; and 5, 6, 7, 9, and 12 days. In addition, young juveniles were fixed at 2, 5, and 7 days after metamorphic loss of the ciliated velar cells. All stages were anesthetized prior to fixation by an initial incubation in artificial seawater containing excess Mg^{2+} and reduced Ca^{2+} concentrations (MgSW: 225 m*M* NaCl, 5 m*M* KCl, 102 m*M* $MgCl_2$, 1 m*M* $CaCl_2$) for 15 min. Vials containing these partially anesthetized larvae were then placed on ice, and drops of a saturated solution of chlorobutanol (Eastman Kodak) in seawater were added to achieve a proportion of 1 part chlorobutanol solution : 4 parts MgSW after 5 min. The anesthetizing solution was then replaced with fixative.

Larvae were fixed at room temperature in 2.5% glutaraldehyde in 0.2 *M* Millonig's phosphate buffer (pH 7.6) and 0.14 *M* sodium chloride for 1 hour, then stored in this fixative for up to 1 week at 10°C. Larval shells were decalcified in a 1:1 mixture of the glutaraldehyde fixative and 10% ethylenediaminetetraacetic acid (disodium salt; Sigma) for no longer than 1 hour (Bonar and Hadfield, 1974). Specimens were then rinsed three times in freshly prepared 2.5% sodium bicarbonate (pH 7.2) and postfixed in 2% osmium tetroxide in 1.25% sodium bicarbonate buffer. Dehydration was accomplished in a graded ethanol series and specimens were embedded in Epon with propylene oxide as the transitional medium.

Histological sections (thickness 0.75 to 1 μm) were cut with glass knives and stained with a mixture of azure II and methylene blue in borax (Richardson *et al.* 1960). Ultrathin sections were cut with a Diatome diamond knife, stained with aqueous 2% uranyl acetate (60 min) and 0.2% lead citrate (6 to 9 min), and photographed with an Hitachi 7000 transmission electron microscope.

Computer-generated reconstructions of sectioned larvae were made with Jandel's PC3D software. Profiles of the body wall (excluding the periostracum covering the decalcified shell) and selected muscles were traced from photomicrographs of sections by using a Numonics digitizing tablet. Sections of 1-μm thickness were traced at intervals of 5 μm, although body wall profiles in the reconstructions that also show underlying muscles are displayed at intervals of 10 μm. The method for aligning photomicrographs of sequential sections has been described by Page (in press).

Results

Larvae of *Haliotis kamtschatkana* hatch from the egg investments at about 30 hours postfertilization (12° to

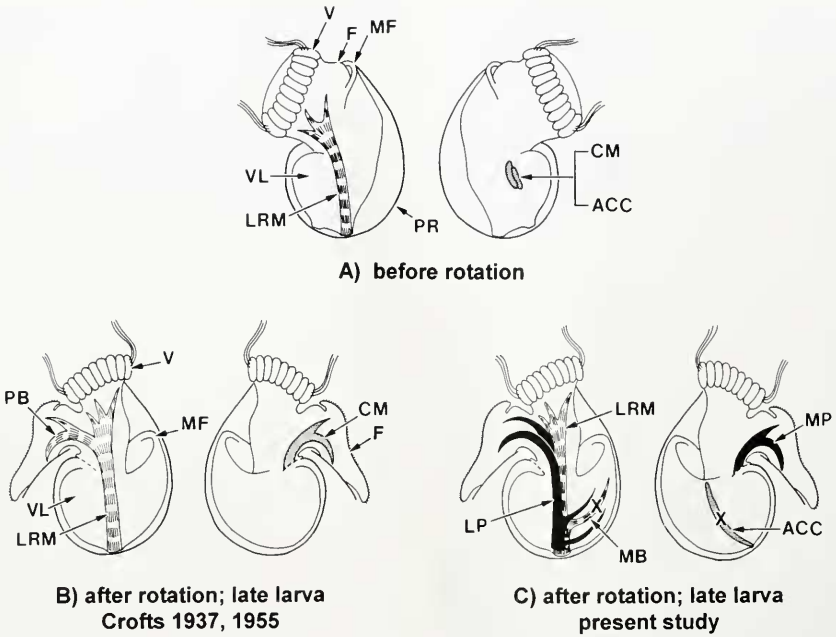

Figure 1. Two interpretations of the larval shell muscles of haliotid gastropods; sketches of muscles are simplified for clarity. (A) Right and left lateral views of a larva before rotation of the cephalopodium relative to the protoconch, showing the larval retractor muscle (LRM) and the muscle identified by Crofts (1937, 1955) as the future columellar muscle (CM) in *Haliotis tuberculata*; the latter muscle is identified as the accessory larval retractor muscle (ACC) in the present study on *H. kamtschatkana*. (B) Crofts' (1937, 1955) interpretation of the shell muscles in a late stage larva of *H. tuberculata* (shown in left and right lateral views); the LRM acquires a pedal branch (PB) and the columellar muscle (CM) projects into the foot. (C) My interpretation of the shell muscles in late stage larva of *H. kamtschatkana* (shown in left and right lateral views); the left and medial pedal muscles (LP, MP) have differentiated, but the ACC and the mantle branch (MB) of the LRM degenerate prior to metamorphosis. Other abbreviations: F = foot; MF = mantle fold; PR = protoconch; V = velum; VL = visceral lobe consisting of differentiating midgut cells.

13°C). At this time, the ovoid larval body has an encircling band of long, compound cilia (velar cilia) that powers swimming, but the foot is not yet recognizable and the protoconch (premetamorphic shell) is merely a small disc. Larvae then undergo rapid and extensive changes in both shape and cellular complexity so as to achieve metamorphic competence by 11 to 12 days postfertilization. They are able to crawl on the foot by 9 days. Major regions of larval anatomy, as referred to in the following text, are labeled on the sketches in Figure 1.

Posthatching development is accompanied by sequential differentiation and subsequent remodeling of four shell-attached muscles. Two of these, which I call the larval retractor muscle (LRM) and the accessory larval retractor muscle (ACC), begin to acquire myofilaments before rotation of the cephalopodium relative to the protoconch and visceral lobe (Fig. 1A), a morphogenetic movement that has been called *ontogenetic torsion*. However, the ACC and the mantle branch of the LRM degenerate prior to metamorphic competence. The other two shell muscles, which I call the left pedal muscle and the medial pedal muscle, differentiate after cephalopodial rotation (Fig. 1C).

Shell muscles can be unambiguously identified by their ultrastructurally distinctive attachment plaque, which is formed by specialized cells of the perivisceral epithelium (Figs. 2 and 3). As shown in Figure 3, the specialized cells are traversed by intracellular filament bundles arising from stubby apical microvilli embedded in the fibrillar matrix of the decalcified protoconch. Mem-

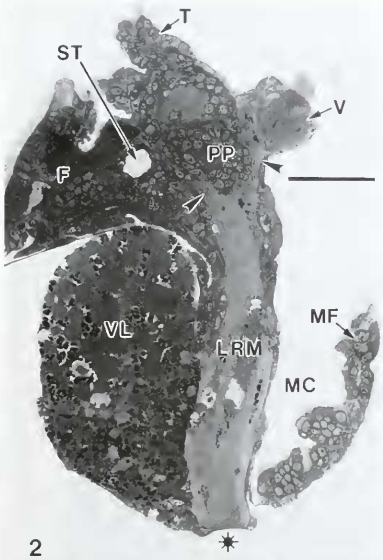

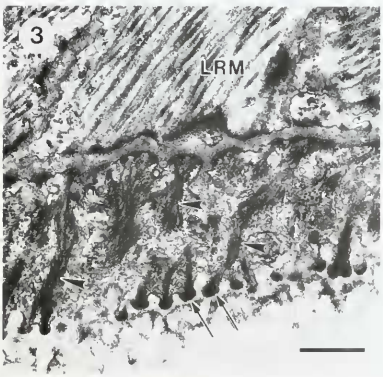

Figure 2. Parasagittal section through a larva of *Haliotis kamtschatkana* at 9 days after fertilization, showing the larval retractor muscle (LRM) projecting anteriorly from its shell attachment plaque (asterisk); distal portions of this muscle (arrowheads) extend into the velum (V) and along the ventral margin of the left pharyngeal pouch (PP). Other abbreviations: F = foot; MC = mantle cavity; MF = mantle fold; ST = statocyst; T = cephalic tentacle, VL = visceral lobe. Scale, 50 μm.

Figure 3. Transmission electron micrograph of a portion of the larval retractor muscle attachment plaque, which consists of specialized perivisceral epithelial cells with intracellular filament bundles (arrowheads) and stubby microvilli (arrows) embedded in the fibrillar matrix of the protoconch (decalcified to allow sectioning). Scale, 0.5 μm.

branes of both the muscle and adjacent epithelial cells have adherens-like junctional specializations that impinge on a thin layer of extracellular matrix lying between these two cell types. Attachment plaques having this morphology have been described previously for both larval and adult gastropods (Bonar, 1978; Tompa and Watabe, 1976).

Larvae also acquire musculature associated with the body wall and differentiating gut. The former consists of a complex network of intrinsic, subepidermal fibers that are particularly abundant within the foot of older larvae. The distal ends of shell muscles connect extensively with intrinsic musculature of the foot and velum. In this report, I do not describe either the gut or intrinsic body wall muscles in detail.

Larval retractor muscle (LRM) and accessory larval retractor muscle (ACC)

The images in Figure 4 are computer-generated reconstructions of transversely sectioned larvae at three stages of development: 52 hours, 5 days, and 9 days postfertilization. The reconstructions show trajectories and developmental changes of the LRM and the ACC, which are described in the following text along with micrographs of selected features.

Before cephalopodial rotation

The protoconch of *H. kamtschatkana* grows rapidly during early development, reaching final size about 52 hours after fertilization. At this stage (Fig. 5), the morphogenetic movement of cephalopodial rotation has either begun or is about to begin. Differentiating myocytes of the LRM and ACC are recognizable in these young larvae (Figs. 6 and 7) because myofilaments can be resolved within the cytoplasm (Fig. 8). Nevertheless, prior to cephalopodial rotation, most of the sarcoplasm is occupied by large yolk inclusions (Fig. 7), and myofilaments are restricted to the extreme distal ends and to a narrow cortical zone beneath the sarcolemma (Fig. 8).

Sections through the mid-level of the visceral lobe at 52 hours show profiles of the ACC and the LRM extending along opposite sides of this yolky mass of differentiating midgut cells (Fig. 6). The LRM consists of eight myocytes, whereas the ACC consists of only two (Fig. 7). No myocytes are added to either of these two muscles during subsequent development.

At 52 hours, two myocytes of the LRM are noticeably larger than the other six, and these two alone make direct contact with shell field epithelial cells that will eventually form the attachment plaque onto the shell. The basal ends of the other six LRM myocytes reach toward the bottom of the shell along the two that establish initial contact with shell field epithelium. In prerotational lar-

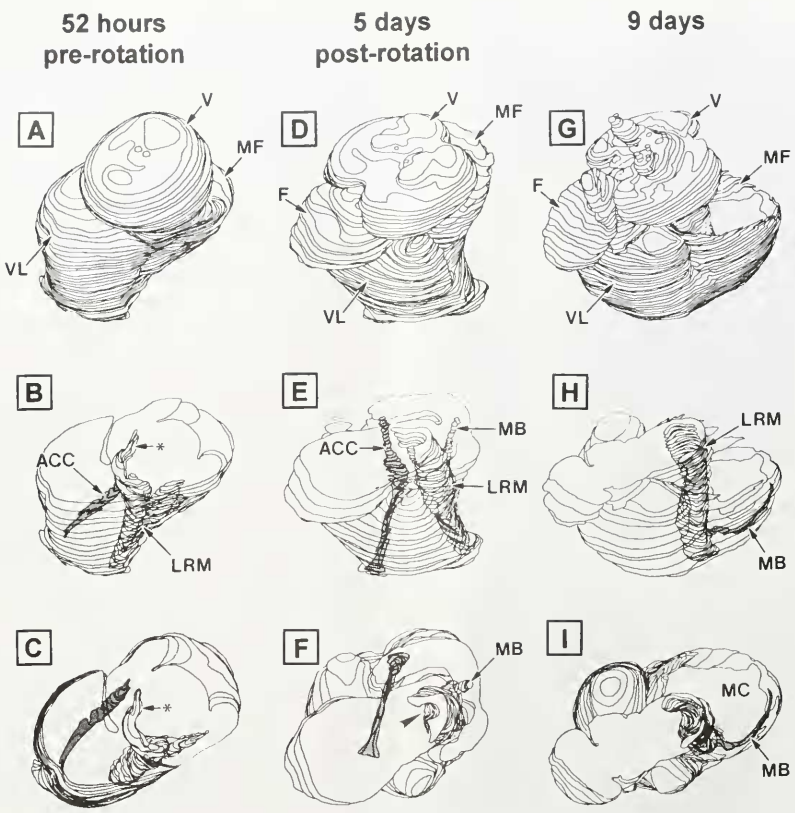

Figure 4. Computer-assisted reconstructions of transversely sectioned larvae at three stages of development (protoconch not included). The upper row shows reconstructions of whole larvae (all viewed from the definitive left lateral side of the visceral lobe) at postfertilization times of 52 hours (A), 5 days (D), and 9 days (G). The middle row (B, E, H) shows the same three stages with the anterior portion omitted and with profiles of the larval retractor muscle (LRM) and accessory larval refractor muscle (ACC) superimposed on the body wall profiles. The lower row (C, F, I) shows the same reconstructions with superimposed muscle profiles, but viewed from the anterior end of the larvae. Asterisk in (B) and (C) indicates the oblique tract of the LRM at 52 hours; arrowhead in (F) indicates the U-shaped excavation in the LRM where it partially surrounds the esophagus. The ACC is stippled in B, C, E, and F; the mantle branch (MB) of the LRM is stippled in H and I. Other abbreviations: F = foot; MC = mantle cavity; MF = mantle fold; V = velum; VL = visceral lobe.

vae, the attachment plaque of the LRM has not acquired the ultrastructural characteristics of its fully differentiated state, as shown in Figure 2, but whole mounts of live larvae suggest that epithelial cells of the future LRM attachment plaque are nevertheless fastened to the inner wall of the shell at this stage (Fig. 5). The attachment site is located at the bottom of the protoconch, but is offset toward one side. The offset is right-sided with respect to the prerotated cephalopodium, but becomes left-sided with respect to the postrotated cephalopodium (Fig. 4: compare A–C with D–F).

The two largest myocytes of the LRM at 52 hours have different distal trajectories. One continues anteriorly along the right side of the foregut and is accompanied by four smaller LRM myocytes. The other of the two largest myocytes bends abruptly to the left, traveling dorsally over the foregut to the opposite side of the larval body. Two additional LRM myocytes show this same oblique

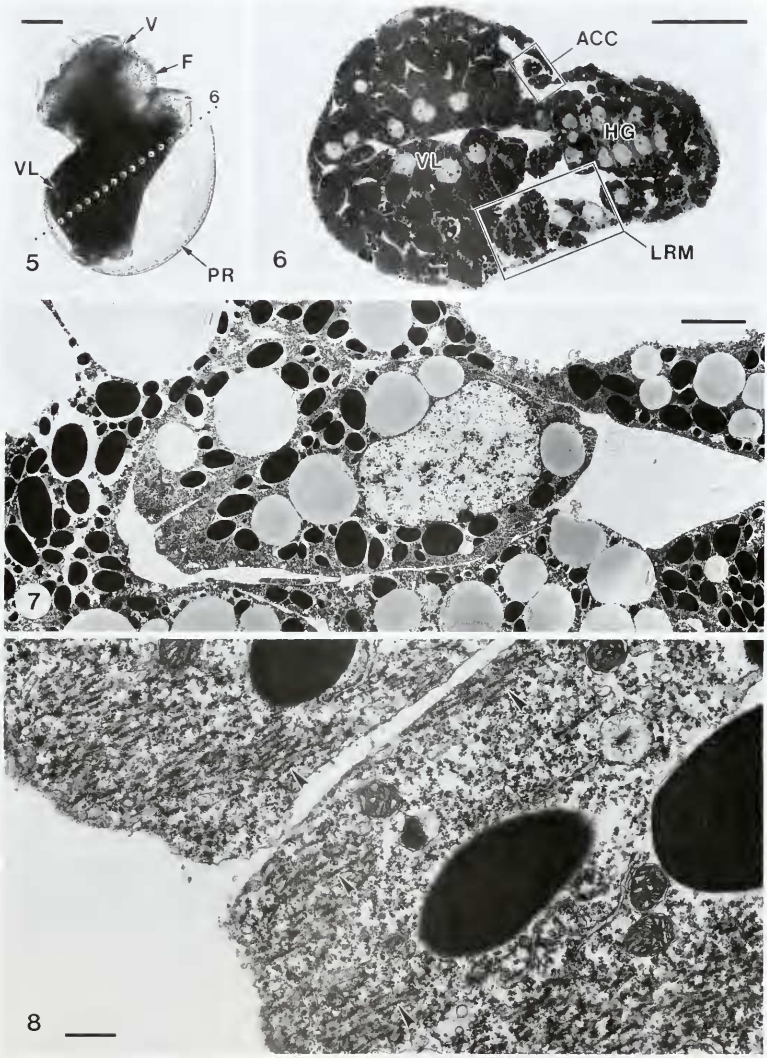

Figure 5–8. Prerotational larvae (52 hours after fertilization).

Figure 5. Lateral view of a live larva; note that the foot rudiment (F) and visceral lobe (VL) are on opposite sides of the body. Dotted line indicates approximate plane of section for Fig. 6. PR = protoconch; V = velum. Scale, 50 μm.

Figure 6. Transverse section through the mid-level of the visceral lobe (VL), showing profiles of the larval retractor muscle (LRM) and the smaller accessory larval retractor muscle (ACC). HG = rudimentary hindgut. Scale, 50 μm.

Figure 7. Transmission electron micrograph (TEM) of the two myocytes of the ACC containing many yolk platelets having two different electron densities. Plane of section is similar to that shown in Fig. 6, but was cut from a different larva. Scale, 5 μm.

Figure 8. TEM showing differentiating myofilaments (arrowheads) within the peripheral cytoplasm of ACC myocytes. Scale, 0.5 μm.

trajectory, which is marked by an asterisk in Fig. 4, B and C. As I have described previously (see fig. 9a, b of Page, in press), the oblique tract of the LRM in prerotational larvae inserts not only on columnar epithelium at the far left side of the foot rudiment (an insertion site described by Crofts [1937] for the oblique tract of the LRM in *Haliotis tuberculata*), but also on adjacent epithelium lining the initial mantle cavity and on shell field epithelium.

Prior to cephalopedal rotation, the distal ends of the two ACC myocytes do not project beyond the visceral lobe of the larval body (Fig. 4B). At 52 hours, the basal ends of these myocytes reach toward their definitive anchorage site on the protoconch, but a differentiated attachment plaque is not yet recognizable.

After cephalopodial rotation

Figure 9 shows a larva of *H. kamtschatkana* at 5 days postfertilization, which is 2 days after the cephalopodium has rotated by 180° relative to the protoconch and visceral lobe (compare the position of the foot relative to the shell in Figs. 5 and 9). As larvae develop beyond the end of the rotation phase, myocytes of the LRM and the ACC enlarge and the proportion of myofilaments relative to yolk inclusions increases dramatically. Concurrently, myofilaments of both muscles become organized into short sarcomeres delimited by rows of Z-bodies (Fig. 10). However, the sarcomeres have a peculiar zig-zag pattern, which may be a fixation artifact imposed on cross-striated fibers that lack strong linkages between adjacent Z-bodies.

At 5 days posthatching, the basal trunks of both the LRM and the ACC can be seen clearly in whole mounted, live larvae (Fig. 9) and in tissue sections (Fig. 11). The attachment plaque of the LRM is located slightly toward the left side of the postrotational shell, whereas the attachment plaque of the ACC has a more ventro-medial location within the bowl of the protoconch.

As shown in the reconstructions in Figure 4, D–F, the trunk of the LRM ascends directly up the left side of the larva from its left-sided attachment plaque, whereas the two muscle cells of the ACC project almost horizontally from their shell attachment plaque so as reach toward the dorso-lateral right side of the visceral lobe. As a result, transverse sections through the extreme base of the visceral lobe cut the LRM in cross-section, but pass through the ACC in oblique longitudinal section (Fig. 11). After reaching the right side, the striated fibers of the ACC continue anteriorly into the right, ventro-lateral area of the mantle fold (Fig. 4, D–F; Figs. 12–15). The ACC extends much further anteriorly at 5 days (postrotational larva) than at 52 hours (prerotational larva).

Upon reaching the proximal level of the developing foregut, six of the eight LRM myocytes remain in close contact and collectively assume a U-shaped cross-sectional profile that invests the dorsal and lateral walls of the esophagus (Figs. 4F, 14). Eventually these six separate into left- and right-sided tracts, which insert on opposite sides of the velum and stomodeal area. The stomodeal fibers also connect with intrinsic muscle fibers extending into the foot.

The other two myocytes of the LRM branch away from the dorsal area of the main muscle bundle and extend into mantle tissue (MB in Figs. 4E, 4F, 14). However, a gradual change in shape of the mantle cavity during the period between the end of cephalopodial rotation and the onset of metamorphic competence forces a change in the disposition of the mantle branch of the LRM. For 2 full days after the cephalopodium has completed its rotation by 180 degrees relative to the protoconch, most of the initial mantle cavity is located along the right side of the larva (Fig. 13). During this initial postrotational period, the mantle branch of the LRM follows a straight anterior trajectory along the mid-dorsal border of this initial mantle cavity (Figs. 4E, 4F, 14). Subsequently, however, the right-sided mantle cavity deepens greatly and its mid-dorsal margin (including the rudiment of the initial ctenidium) pushes over to the left side, thereby creating a broad, mantle-lined cavity over the dorsal area of the body (Fig. 4, G–I; Fig. 16). As this happens, the mantle branch of the LRM is forced to diverge from the main muscle bundle at a more posterior level, and the branch becomes a curved arc that embraces the far wall of the much enlarged mantle cavity (compare Fig. 4, F and I; also Figs. 14 and 17).

The two myocytes of the ACC and the two myocytes of the mantle branch of the LRM, both of which project into the mantle fold, do not survive to the end of the obligatory larval period. In sections through larvae fixed at 9 days postfertilization, myocytes of the ACC are absent altogether or appear as a globular mass at the base of the visceral lobe. The mantle branch of the LRM is present at 9 days but not at 12 days postfertilization.

Left and medial pedal muscles

At the onset of cephalopodial rotation at 52 hours, the foot rudiment is merely a low swelling immediately beneath the stomodeum, although a small, thin operculum is present. However, dramatic enlargement of the foot begins during cephalopodial rotation and continues through the remainder of the obligatory larval period. During the initial enlargement, the foot becomes filled with a proliferating mass of cells. By 4 days postfertilization (24 hours after the end of cephalopodial rotation), occasional aggregations of myofilaments can be resolved within some of these pedal cells. Sections through pro-

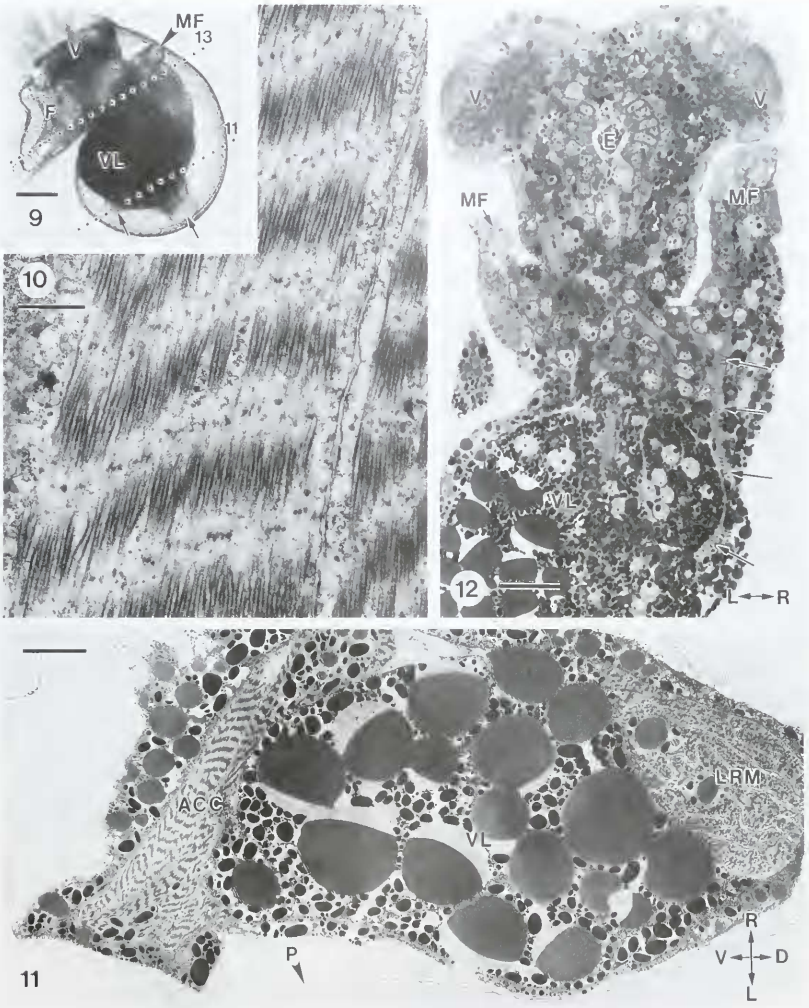

Figures 9–12. Postrotational larvae at 5 days after fertilization.

Figure 9. Lateral view of live larva; enlarged foot (F) now projects on same side as the visceral lobe (VL). Shell attachments of the larval retractor muscle (LRM) and the accessory larval retractor muscle (ACC) are indicated by arrows. Planes of section for Figs. 11 and 13 are indicated by dotted lines. MF = mantle fold; V = velum. Scale, 50 μm.

Figure 10. Transmission electron micrograph (TEM) of striated myofilament arrangement within a myocyte of the ACC. Scale, 1 μm.

Figure 11. TEM of a transverse section that passes through the basal trunks of both the LRM and ACC. P = periostracum of decalcified protoconch; VL = visceral lobe. Orientation axes: V = ventral; D = dorsal; R = right; L = left. Scale, 10 μm.

Figure 12. Frontal section showing the striated myofilaments of the ACC (arrows) extending anteriorly into the ventro-lateral right side of the mantle fold (MF). E = developing esophagus; MF = mantle fold; V = velum; VL = visceral lobe. Orientation axes: L = left; R = right. Scale, 50 μm.

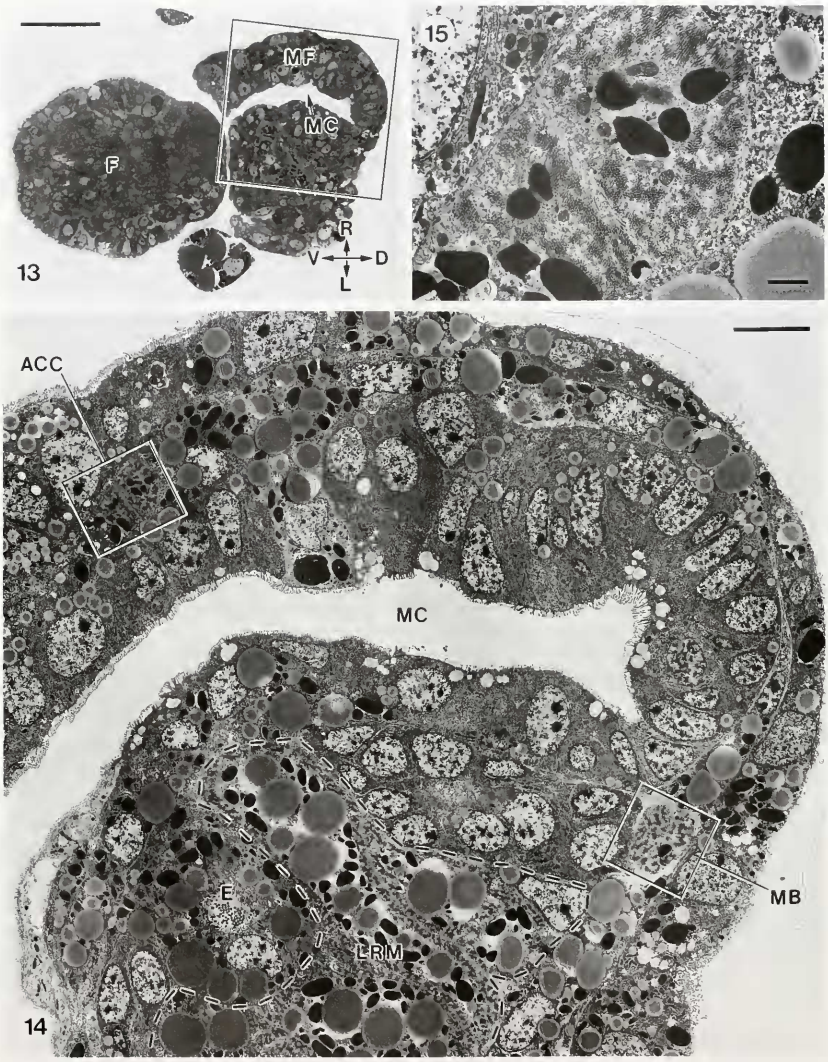

Figures 13–15. Postrotational larvae at 5 days after fertilization.

Figure 13. Transverse section along the plane indicated in Fig. 9 and passing through the foot (F) and the mantle fold (MF) bordering the deep mantle cavity (MC) on the right side. Boxed area shown in Fig. 14. Orientation axes: D = dorsal; V = ventral; L = left; R = right. Scale, 50 μm.

Figure 14. Transmission electron micrograph (TEM) of boxed area in Fig. 13 (cut from different larva); dashed lines outline a portion of the main body of the larval retractor muscle (LRM) that partially surrounds the developing esophagus (E). The section also shows the accessory larval retractor muscle (ACC) within the right-sided mantle fold (enlarged in Fig. 15) and the mantle branch (MB) of the LRM located mid-dorsally. MC = mantle cavity. Scale, 1 μm.

Figure 15. Enlargement of the ACC from Fig. 14. Scale, 1 μm.

Figure 16. Transverse section of larva at 9 days after hatching, showing the enlarged mantle cavity (MC); boxed area is shown in Fig. 17. MF = mantle fold; VL = visceral lobe. Orientation axes: D = dorsal; V = ventral; L = left; R = right. Scale, 50 μm.

Figure 17. Transmission electron micrograph (TEM) of boxed area in Fig. 16 (cut from different larva), showing the main body of the LRM and its mantle branch (slender arrows). The left pedal muscle (stout arrow) extends along the left side of the LRM and has a denser myoplasm than the LRM. Scale, 10 μm.

gressively older larval stages suggest that the pedal myoblasts give rise to intrinsic pedal muscles and possibly to two shell-attached pedal muscles, which I call the left pedal muscle and the medial pedal muscle.

The arrangement of myofilaments within the two pedal muscles is similar, but is different from that found for the LRM and ACC. Pedal muscles have much longer thick filaments and do not show obvious striations (Figs. 18–20).

The two pedal muscles have different shell-attachment sites and trajectories. The left pedal muscle is attached to the posterior area of the left side of the protoconch, and its trunk travels anteriorly along the ventro-lateral left side of the LRM (Fig. 17). Before entering the foot, the

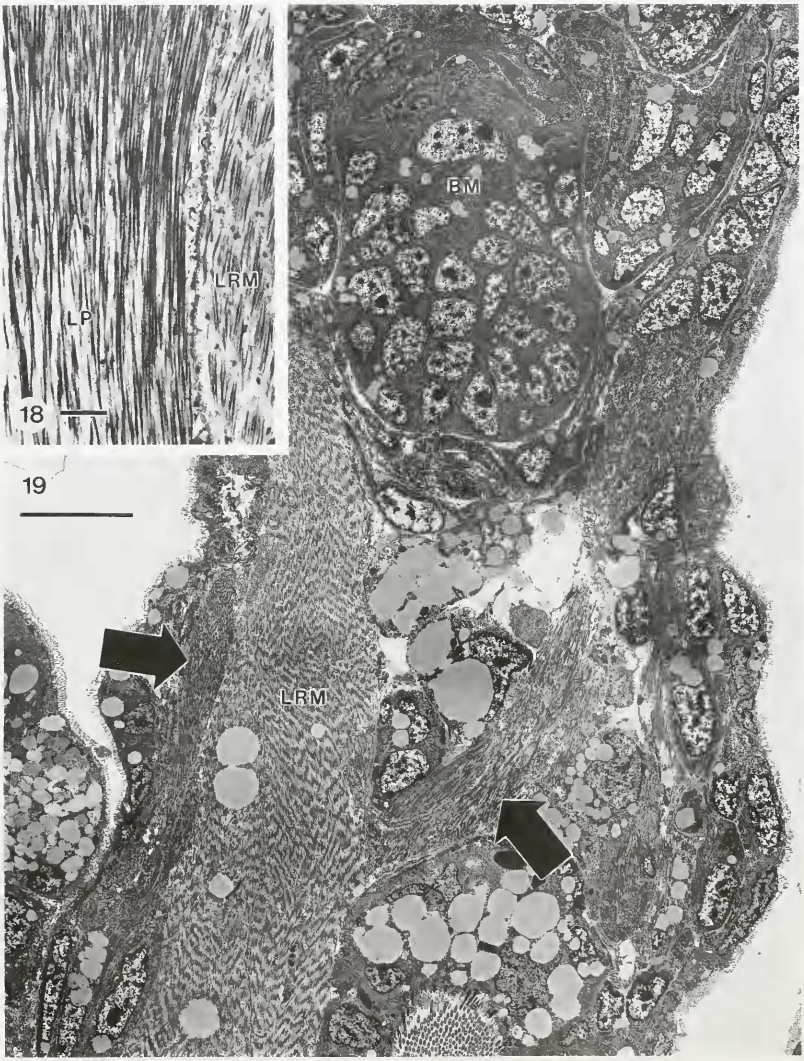

Figure 18. Transmission electron micrograph (TEM) showing different myofilament arrangements in myocytes of the left pedal muscle (LP) and the larval retractor muscle (LRM). Scale, 1 μm.

Figure 19. TEM of a frontal section through a 12-day larva, showing the ipsilateral and contralateral distal branches (arrows) of the left pedal muscle. Unlike the LRM, the left pedal muscle does not show obvious striations. BM = buccal mass. Scale, 10 μm.

left pedal muscle bifurcates into two distal branches (Fig. 19). One branch extends into the left (ipsilateral) side of the foot, whereas the other extends into the right (contralateral) side of the foot. Therefore, sagittal sections through larvae pass obliquely through the contralateral branch of the left pedal muscle as it reaches toward the

right side of the foot (Fig. 20). Although the foot is the primary target of the left pedal muscle, this muscle also includes slender muscle slips that extend into the mantle fold.

The medial pedal muscle of late stage larvae is anchored on the external surface of a calcareous septum that is secreted along the visceral margin of the protoconch (Figs. 20 and 21); the septum is described in greater detail by Page [in presss]). The muscle arches over the junction between the visceral rim of the protoconch and the operculum and extends into the central area of the foot. The various fibers of the medial pedal muscle insert on pedal epithelium underlying the operculum, on intrinsic muscle fibers associated with the crawling surface of the foot, and on the large propodial gland.

Shell muscles after metamorphosis

Sections through young juveniles at 2 to 7 days postmetamorphosis show that both pedal muscles are retained through metamorphosis and the mantle fibers of the left pedal muscle become more prominent (Fig. 22). However, the LRM, which lost the two myocytes of the mantle branch prior to metamorphosis, continues to lose myocytes after metamorphosis. Juveniles sectioned at 7 days after metamorphosis have only two LRM myocytes (Fig. 23).

By 7 days postmetamorphosis, the attachment plaque of the left pedal muscle has migrated anteriorly along the left wall of the protoconch. Also at this time, the right border of the medial pedal muscle has spread onto the right flank of the protoconch. This spreading may represent an early stage in the migration of the medial pedal muscle to the dorsal surface of the ear-shaped teleoconch, so as to eventually become the larger of the two shell muscles in adult abalone.

Discussion

Inventory of larval shell muscles: comparison to accounts by Crofts and others

Muscle morphogenesis in *Haliotis kamtschatkana* is a dynamic process that incorporates both temporal and spatial changes during the course of development. During the developmental interval that I examined, I noted differences in the time when myofilaments appeared within cells of individual muscles, and changes in details of distal insertions, migration of shell attachment plaques, and differential expression of myocyte destruction programs. However, remodeling is secondary to the fact that four shell muscles differentiate during the larval phase, and these four fall into two broad categories based on structural, functional, and developmental criteria.

One category consists of the LRM and ACC, which collectively retract the head and mantle in postrotational larvae. The striated myofibers of these two muscles begin to form before cephalopodial rotation; they differentiate from progenitor cells lying on either side of the yolky mass of differentiating midgut cells. The ACC and the mantle branch of the LRM, which both insert within the mantle fold, degenerate prior to metamorphic competence.

The second category of larval shell muscles consists of two pedal muscles. These two, together with the intrinsic musculature of the foot, may arise from progenitor cells within the foot rudiment, but this requires confirmation from cell labeling studies. The pedal muscles become recognizable only after cephalopodial rotation, and both muscles lack obvious striations. However, the medial pedal muscle is anchored on a calcareous septum secreted along the visceral rim of the shell aperture, whereas the left pedal muscle reaches posteriorly along the left side of the LRM and attaches to the postero-lateral wall of the protoconch (offset toward the left side). The medial and left pedal muscles function to pull the foot into the shell cavity during larval retraction, and their differentiation correlates with the period of rapid foot enlargement. The pedal muscles must also function to brace the shell over the foot during crawling, a behavior that emerges 9 days after fertilization (12° to 13°C) and is promoted by either red coralline algae or 0.01 m*M* gamma aminobutyric acid.

When Crofts (1937, 1955) did her classic studies of larval development and muscle morphogenesis in *Haliotis tuberculata* and several other archaeogastropods, her analysis was restricted to observations on live larvae and paraffin sections and she was not able to prevent muscle contraction during chemical fixation (Crofts, 1937, p. 221). Improved methods, particularly electron microscopy and effective neuromuscular anesthetics, permit greater resolution of the pattern of muscle development. Although the larval shell muscles and their distal branches are theoretically resolvable by light microcopy, the high degree of structural complexity that is packed into a very small volume makes many structural details difficult to identify. I suggest that Crofts (1937, 1955) made some errors concerning the larval shell muscles of haliotids, which may have led to inappropriate interpretations of the ancestral homologues of these muscles. Nevertheless, because Crofts' descriptions and camera lucida sketches are detailed and meticulous within the limits of her technique, it is possible to identify the probable sources of discrepancy between her observations on *H. tuberculata* and the results reported here for *H. kamtschatkana*.

Most importantly, Crofts (1937, 1955) may have misidentified the ACC in prerotational larvae as an early

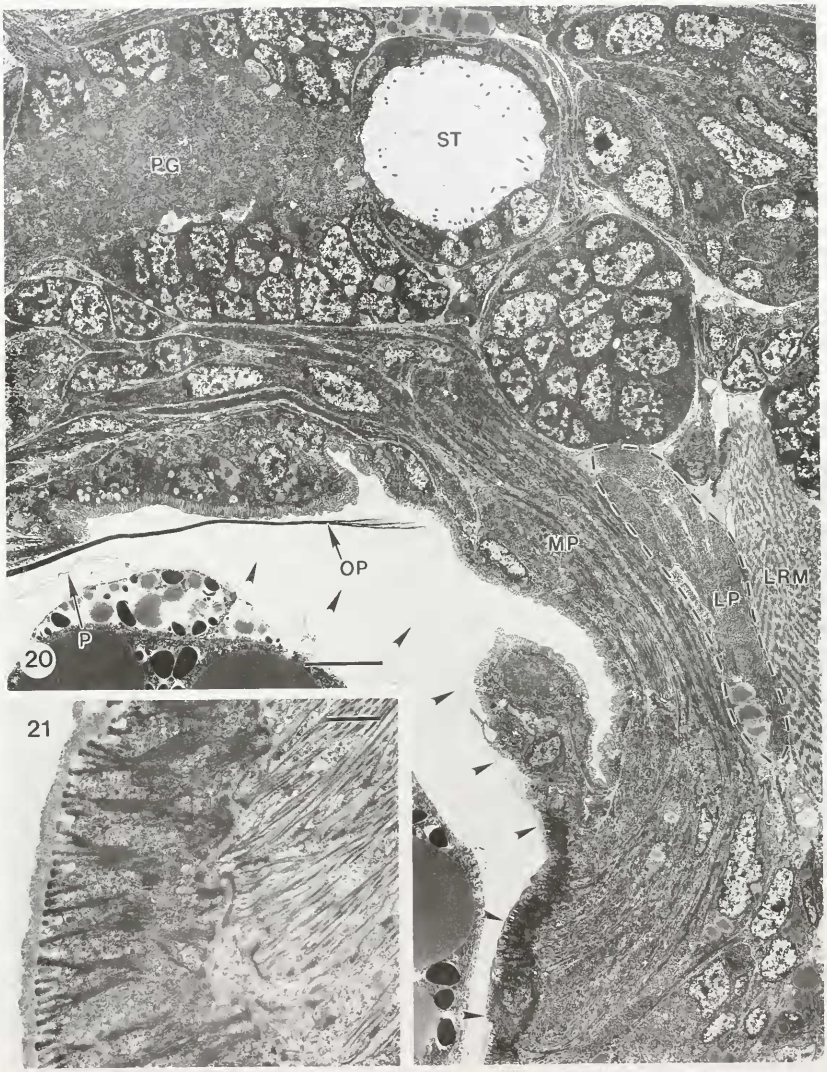

Figure 20. Transmission electron micrograph (TEM) of a longitudinal section through the base of the larval foot at 12 days after fertilization. Note the medial pedal muscle (MP) extending into the foot from an anchorage site on a calcareous shelf at the ventral apertural lip of the protoconch (arrowheads indicate decalcified matrix of septum). The section passes obliquely through the contralateral branch of the left pedal muscle (LP; outlined by dashed lines) and a small portion of the larval retractor muscle (LRM). OP = operculum; P = periostracum of decalcified protoconch; PG = right pedal ganglion; ST = right statocyst. Scale, 10 μm.

Figure 21. TEM showing enlarged view of the attachment plaque of the medial pedal muscle. Scale, 1 μm.

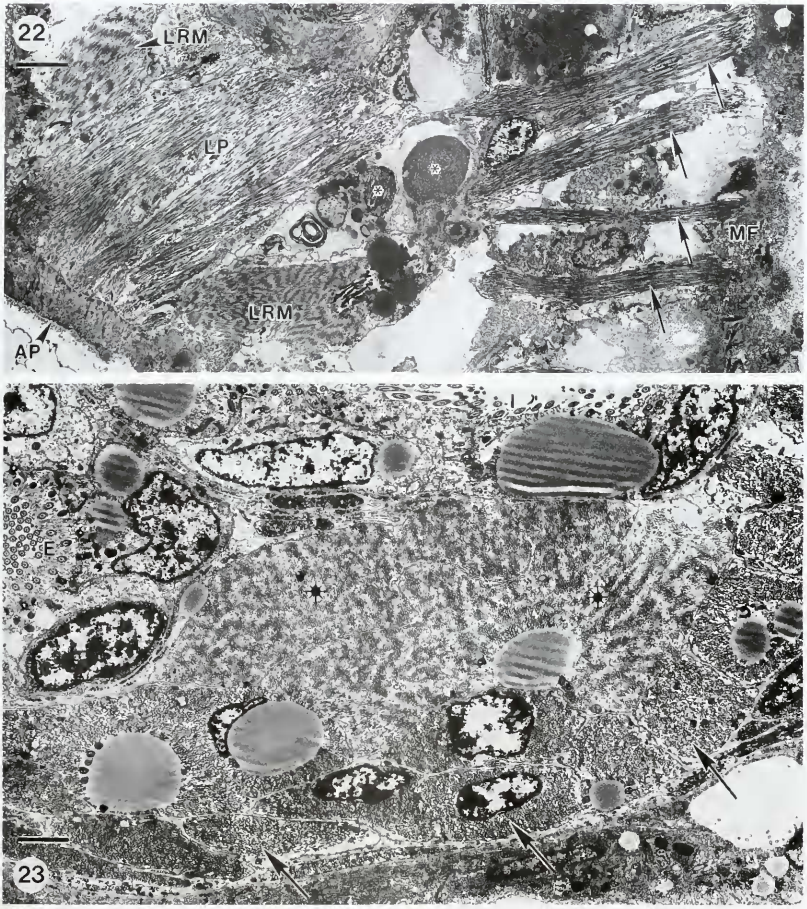

Figure 22. Transmission electron micrograph (TEM) of a sagittal section through the extreme left side of a postlarva at 2 days after velum loss; the section passes through the left side of the mantle fold (MF) and the shell-attached trunk of the left pedal muscle (LP). Digit-like muscle processes (arrows) extend from the LP into the mantle fold; asterisks indicate degenerating myocytes. AP = shell-muscle attachment plaque; LRM = myocytes of the larval retractor muscle. Scale, 5 μm.

Figure 23. TEM of a transverse section through the LRM and left pedal muscle in a juvenile at 7 days after metamorphic loss of the velar cilia; the section passes through the left pedal muscle (arrows) where the contralateral branch is diverging from the ipsilateral branch. Only two LRM myocytes (asterisks) remain at this stage. E = esophagus; I = intestine. Scale, 2 μm.

stage in the morphogenesis of the medial pedal muscle. She used the terms *columellar muscle* or *post-torsional right shell muscle* for both. Crofts stated: "Early in the second day [*i.e.*, before cephalopodial rotation] there are invariably two spindle-shaped cells derived from the left mesoderm band. They are about one-third the length of the muscle cells of the right side and have no shell attachment" (Crofts, 1937, p. 230). She refers to a camera lucida sketch (fig. 25 of Crofts, 1937) of a transverse section in which the two mesoderm cells are identified as the ru-

diment of the columellar muscle. Her sketch is comparable to the section shown in my Figure 6, which also shows two myoblasts on the left side of the developing midgut. However, in *H. kamtschatkana*, these two are differentiating myocytes of the ACC, which is an entirely different muscle from the later-differentiating columellar muscle (= medial pedal muscle). The ACC of *H. kamtschatkana* soon acquires an attachment to the bottom of the protoconch and projects into the right, ventro-lateral area of the mantle fold. Indeed, the shell-attached trunks of both the ACC and the LRM can be seen for several days after larvae complete cephalopodial rotation (Fig. 9). However, Crofts (1995, p. 729) vigorously disputed a previous report on larvae of *Patella vulgata* by Smith (1935), in which he described two distinct muscles attached to separate sites along the bowl of the protoconch. However, Bandel (1982) has also reported two muscles attached to the bottom of the protoconch in early developmental stages of several trochacean archaeogastropods. One of these is clearly comparable to the LRM of haliotid larvae; the other is somewhat similar to the ACC, except that Bandel's (1982) text fig. 5 gives it a distal trajectory that is more like that of the mantle branch of the LRM in *H. kamtschatkana*.

In her 1937 paper (p. 238) Crofts states that the LRM of older larvae of *H. tuberculata* "acquires additional spindle-like fibres extending into the left side of the foot." This description may correspond to what I have identified as the distal, ipsilateral tract of the left pedal muscle in *H. kamtschatkana*. The contralateral tract, which extends into the right side of the foot, is difficult to resolve in light microscopical sections because it branches from the muscle trunk in a very structurally congested area of the larval body. Crofts interpreted these "additional fibres" as merely an elaboration of the LRM, but I suggest that they should be identified as a distinct shell muscle. Although both the left pedal muscle and the LRM attach to the shell along the left side of the bottom of the protoconch, the two muscles are different in all other respects that I could identify, including (1) temporal pattern of myofilament differentiation, (2) primary insertion target, and (3) type of myofilament arrangement.

In summary, I suggest that Crofts (1937, 1955) may have overlooked the existence of what are actually two categories of shell muscles in haliotid larvae. Specifically, she may have misidentified the ACC as an early stage in the development of the medial pedal muscle (columellar muscle) and she may not have distinguished the left pedal muscle as separate from the LRM (Fig. 1). My suggestion could be falsified by an ultrastructural reanalysis of shell muscle development in *H. tuberculata*. It is possible that muscle development in *H. tuberculata* and *H. kamtschatkana* show real and profound differences.

Comparisons to larval shell muscles in other gastropods

Ultrastructural information on the shell muscles of other gastropod larvae is available only for members of the Nudibranchia (Bonar and Hadfield, 1974; Page, 1995). These studies reveal a common groundplan for nudibranch larval shell muscles that is similar to the pattern seen for *H. kamtschatkana* larvae. The two pedal muscles and the LRM in *H. kamtschatkana* have similar counterparts in nudibranch larvae, and in each case the LRM differentiates before the pedal muscles. However, nudibranch larvae appear to lack the ACC. Nevertheless, the nudibranch LRM incorporates a tract that projects to the right, ventro-lateral part of the right mantle fold, which is the target of the ACC in *H. kamtschatkana*. Another notable difference between the shell muscles in *H. kamtschatkana* larvae and those of nudibranch larvae is the lack of a mid-ventral stomodeal tract in the LRM of *H. kamtschatkana*.

Existing studies on caenogastropod larvae consistently describe only one shell-attached muscle (*e.g.*, Werner, 1955; D'Asaro, 1965, 1966, 1969; Fioroni, 1966; Fretter, 1969, 1972; Fretter and Graham, 1962; Thiriot-Quievreux, 1969, 1974). This muscle initially attaches to the left side of the protoconch, but later transfers to the columella of the growing larval shell. The single shell muscle is reported to have distal branches inserting on the velum, distal foregut structures, mantle fold, and foot.

Ancestral homologues of haliotid larval shell muscles

I have categorized larval shell muscles in *H. kamtschatkana* according to characteristics of structure, function, and spatial and temporal patterns of myofibrillogenesis. These criteria delineate two categories of larval shell muscles: (1) early-differentiating cephalic and mantle retractors consisting of striated myofibers, and (2) later-differentiating pedal and mantle muscles consisting of myofibers that lack obvious striations. However, previous descriptions of shell muscles in larval archaeogastropods attempted to categorize larval shell muscles according to possible left–right homologues, and the search carried the *a priori* expectation that the homologues would show anatomical differences (see Haszprunar 1985, 1988). The reason can be traced to a preexisting evolutionary scenario for gastropods, as popularized by Garstang (1929), who proposed that gastropod torsion was the result of a mutation that created an asymmetry between left and right larval shell muscles. The hypothesized asymmetry was such that the cephalopodium of the larval body was made to twist relative to the visceropallium (*i.e.*, the larval body underwent torsion). Garstang (1929) further suggested that this ancient evolutionary event has been preserved over many millenia and is manifest today in the ontogeny of extant

archaeogastropods. Garstang's theory about the evolutionary generation of torsion has had great impact on interpretations of gastropod evolution and phylogeny, although other aspects of his theory, including his functional interpretation of ontogenetic torsion, have been criticized by subsequent authors (Ghiselin, 1966; Thompson, 1967; Salvini-Plawen, 1980; Pennington and Chia, 1985).

Nevertheless, Garstang's (1929) theory for the evolution of torsion and the role of muscles in the torsional process was the conceptual backdrop for Crofts' (1937, 1955) interpretation of shell muscles in larval archaeogastropods. Accordingly, she proposed that the LRM and ACC are left–right homologues showing marked asymmetry in size, trajectory, and time of development. This interpretation is not disproved by the observations reported here. However, by suggesting that the ACC *becomes* the columellar muscle (posttorsional right shell muscle) in *H. tuberculata* and other archaeogastropods, Crofts established the precedent for the view that (1) haliotid larvae have only two shell muscles, (2) these are bilateral homologues that become the two postmetamorphic shell muscles, and (3) the two postmetamorphic shell muscles are therefore homologues of a single pair of dorso-ventral shell muscles in chitons (and presumably monoplacophorans). This interpretation is now shown to be suspect. In *H. kamtschatkana*, the LRM and medial pedal muscle belong to separate muscle groups. If the medial pedal muscle has a homologue in these larvae, the left pedal muscle is a more likely candidate than the LRM.

How can any hypothesis about bilateral muscle homologues and their role in torsion be tested (much less disproved) if both structural and developmental differences are barred from consideration because differences are actually specified by the evolutionary theory about torsion? One way out of circular arguments on this topic is to collect highly resolved morphological data on larval shell muscles for many different gastropod groups and for outgroups. Comparative developmental studies may allow muscle homologues to be identified in a way that is independent of any prevailing evolutionary theory about torsion.

Acknowledgments

I thank Cathy and Joachim Schnorr von Carolsfeld of West Wind Sealab Supply for collecting adult abalone and Canadian Department of Fisheries and Oceans for issuing the collection permit. Comments by Dr. Carole Hickman and an anonymous reviewer were very helpful. This study was funded by a research grant to the author from the Natural Sciences and Engineering Research Council of Canada.

Literature Cited

Bandel, K. 1982. Morphologie und Bildung der frühontogenetischen Gehäuse bei conchiferen Mollusken. *Facies (Erlangen)* **7:** 1–198.

Bonar, D. B. 1978. Fine structure of muscle insertions on the larval shell and operculum of the nudibranch *Phestilla sibogae* (Mollusca: Gastropoda) before and during metamorphosis. *Tissue Cell* **10:** 143–152.

Bonar, D. B., and M. G. Hadfield. 1974. Metamorphosis of the marine gastropod *Phestilla sibogae* Bergh (Nudibranchia: Aeolidacea). I. Light and electron microscopic analysis of larval and metamorphic stages. *Biol. Bull.* **165:** 119–138.

Crofts, D. R. 1937. The development of *Haliotis tuberculata*, with special reference to the organogenesis during torsion. *Philos. Trans. R. Soc. Lond.* **B228:** 219–268.

Crofts, D. R. 1955. Muscle morphogenesis in primitive gastropods and its relation to torsion. *Proc. Zool. Soc. Lond.* **125:** 711–750.

D'Asaro, C. N. 1965. Organogenesis, development and metamorphosis in the queen conch, *Strombus gigas*, with notes on the breeding habits. *Bull. Mar. Sci. Gulf Caribb.* **15:** 359–416.

D'Asaro, C. N. 1966. The egg capsules, embryogenesis, and early organogenesis of a common oyster predator, *Thais haemostoma floridana* (Gastropoda, Prosobranchia). *Bull. Mar. Sci. Gulf Caribb.* **16:** 884–914.

D'Asaro, C. N. 1969. The comparative embryogenesis and early organogenesis of *Bursa corrugata* Perry and *Distorsio clathrata* Lamarck (Gastropoda, Prosobranchia). *Malacologia* **9:** 349–389.

Fioroni, P. 1966. Zur Morphologie und Embryogenese des Darmtraktes und der transitorischen Organe bei Prosobranchiern (Mollusca, Gastropoda). *Rev. Suisse Zoo.* **73:** 621–876.

Fretter, V. 1969. Aspects of metamorphosis in prosobranch gastropods. *Proc. Malacol. Soc. Lond.* **38:** 375–386.

Fretter, V. 1972. Metamorphic changes in the velar musculature, head and shell of some prosobranch veligers. *J. Mar. Biol. Assoc. U.K.* **52:** 161–177.

Fretter, V., and A. Graham. 1962. *British Prosobranch Molluscs.* Ray Society, London.

Garstang, W. 1929. The origin and evolution of larval forms. *Rep. Brit. Assoc. Adv. Sci.* **Section D:** 77–98.

Ghiselin, M. T. 1966. The adaptive significance of gastropod torsion. *Evolution* **20:** 337–348.

Harper, J. A., and H. B. Rollins. 1982. Recognition of Monoplacophora and Gastropoda in the fossil record: a functional morphological look at the bellerophont controversy. *Proc. Third N. Amer. Paleont. Conv.* **1:** 227–232.

Haszprunar, G. 1985. On the innervation of gastropod shell muscles. *J. Moll. Stud.* **51:** 309–314.

Haszprunar, G. 1988. On the origin and evolution of major gastropod groups with special reference to the Streptoneura. *J. Moll. Stud.* **54:** 367–441.

Haszprunar, G. 1993. The Archeogastropoda. A clade, a grade or what else? *Am. Malacol. Bull.* **10:** 165–177.

Hickman, C. S. 1988. Archaeogastropod evolution, phylogeny, and systematics: a re-evaluation. *Malacol. Rev. Suppl.* **54:** 367–441.

Knight, J. B. 1952. Primitive fossil gastropods and their bearing on gastropod evolution. *Smithson. Misc. Coll.* **117:** 1–56.

Morse, D. E., H. Duncan, N. Hooker, and A. Morse. 1976. Hydrogen peroxide induces spawning in mollusks, with activation of prostaglandin endoperoxide synthetase. *Science* **196:** 298–300.

Morse, D. E., N. Hooker, H. Duncan, and L. Jensen. 1979. Gamma aminobutyric acid, a neurotransmitter, induces planktonic abalone larvae to settle and begin metamorphosis. *Science* **204:** 407–410.

Morse, D. E., and A. Morse. 1984. Recruitment and metamorphosis of *Haliotis* larvae induced by molecules uniquely available at the surfaces of crustose red algae. *J. Exp. Mar. Biol. Ecol.* **75:** 191–215.

Page, L. R. 1995. Similarities in form and developmental sequence for three larval shell muscles in nudibranch gastropods. *Acta Zool. (Stockholm)* **76:** 177–191.

Page, L. R. in press. Ontogenetic torsion and protoconch form in the archaeogastropod *Haliotis kamtschatkana*: evolutionary implications. *Acta Zool. (Stockholm).*

Pennington, J. R., and F. S. Chia. 1985. Gastropod torsion: a test of Garstang's hypothesis. *Biol. Bull.* **169:** 391–396.

Richardson, K. D., L. Jarret, and E. H. Finke. 1960. Embedding in epoxy resins for ultrathin sectioning in electron microscopy. *Stain Technol.* **35:** 313–323.

Runnegar, B., and J. Pojeta, Jr. 1985. Origin and diversification of the Mollusca. Pp. 1–57 in *The Mollusca*, K. M. Wilbur, ed., v. 10, *Evolution* E. R. Trueman and M. R. Clarke, eds. Academic Press, New York.

Salvini-Plawen, L. 1980. A reconsideration of the systematics in the Mollusca (phylogeny and higher classification). *Malacologia* **19:** 249–278.

Smith, F. G. W. 1935. The development of *Patella vulgata*. *Philos. Trans. R. Soc. Lond.* **B225:** 95–125.

Stasek, C. R. 1972. The molluscan framework. Pp. 1–44 in *Chemical Zoology*, M. Florkin and B. T. Scheer, eds. Academic Press, New York.

Thiriot-Quiévreux, C. 1969. Organogénèse larvaire du genre *Atlanta* (Mollusque Heteropode). *Vie Milieu* **20:** 347–396.

Thiriot-Quiévreux, C. 1974. Anatomie interne de véligeres planctoniques de Prosobranches Mesogastropodes au stade proche de la métamorphose. *Thalassia Jugosl.* **10:** 379–399.

Thompson, T. E. 1967. Adaptive significance of gastropod torsion. *Malacologia* **5:** 423–430.

Tompa, A. S., and N. Watabe. 1976. Ultrastructural investigation of the mechanism of muscle attachment to the gastropod shell. *J. Morphol.* **149:** 339–352.

Werner, B. 1955. Uber die Anatomie, die Entwicklung und Biologie des Veligers und der Veliconcha von *Crepidula fornicata* (L.) (Gastropoda, Prosobranchia). *Helgol. Wiss. Meeresunters.* **5:** 169–217.

Wingstrand, K. G. 1985. On the anatomy and relationships of recent Monoplacophora. *Galathea Report* **16:** 7–94.

Yochelson, E. L. 1967. Quo vadis *Bellerephon?* Pp. 141–161 in *Essays in Paleontology and Stratigraphy*, C. Teichert and E. L. Yochelson, eds. The University of Kansas Press, Lawrence, Kansas.